A Compensator to Advance Gyro-Free INS Precision

Chao-Yu Hung, Chun-Min Fang, and Sou-Chen Lee

Abstract: The proposed inertial measurement unit (IMU) is composed of accelerometers only. It can determine a vehicle's position and attitude, which is the Gyro-free INS. The Gyro-free INS error is deeply affected by the sensor bias, scale factor and misalignment. However, these parameters can be obtained in the laboratory. After these misalignments are corrected, the Gyro-free strap-down INS could be more accurate. This paper presents a compensator design for the strap-down six-accelerometer INS to correct misalignment. A calibration experiment is taken to get the error parameters. A simulation results show that it will decrease the INS error to enhance the performance after compensation.

Keywords: Calibration, compensator, gyro-free INS, misalignment.

1. INTRODUCTION

The inertial navigation system (INS) is designed to obtain the vehicle dynamic states. The INS is a self-contained system which does not need other information or additional instrumentation [1,2]. The Gyro-free INS which is without a gyroscope equipment is used to determine the velocity, position and attitude of a vehicle in motion. To use linear accelerometers to measure a moving vehicle was first proposed by Schuler in 1967 [3]. Schuler proposed a moving vehicle analysis method requested at least nine accelerometers. A novel scheme, using just six accelerometers, was proposed by Chen [4]. The accelerations of rotation and location of a vehicle were computed using six accelerometer measurements.

The error effect is an important factor in INS. However the misalignment is an important error source for a six-accelerometer INS. The error of six-accelerometer INS is sensitive to time. In 2000, Mostov applied Chen's theory to design a Gyro-free inertial navigation system and then proposed a method to estimate the system errors [5]. This research provides a calibration method to obtain the misalignment and a compensator design for compensating the misalignment of six-accelerometer INS. After compensate, the navigation accuracy of six-accelerometer scheme will be improved obviously.

Manuscript received July 18, 2005; revised February 9, 2006; accepted February 27, 2006. Recommended by Editorial Board member Jae Weon Choi under the direction of Editor Keum-Shik Hong. This research was supported by the National Science Council, NSC-94-2212-E-262-005-. This support is gratefully acknowledged.

Chao-Yu Hung and Chun-Min Fang are with the Department of System Engineering, Chung Cheng Institute of Technology, National Defense University, Ta-shi, Tao-yuan County 335, Taiwan, R.O.C. (e-mails: {g940405, g930405} @ccit.edu.tw).

Sou-Chen Lee is with the College of Electrical Engineering and Computer Science, Lunghwa University of Science and Technology, 300, Sec. 1, Wanshou Rd., Gueishan Shiang, Tao-yuan County 333, Taiwan, R.O.C. (e-mail: sclee@mail.lhu.edu.tw).

2. NAVIGATION EQUATION

2.1. Time derivative for the direction cosine matrix

Consider a time-variant direction cosine matrix, $C_b^i(t)$ that transforms a column matrix from body coordinates, b, into inertial coordinates, i. The geometry of the body-frame and inertial-frame are shown as Fig. 1.

The time derivative for the direction cosine matrix can be expressed as [6]

$$\dot{C}_b^i = C_b^i\left[\vec{\omega}_{ib}^b \times\right]. \tag{1}$$

2.2. Position equation

In Fig. 1, we define the relationship between body-frame and inertial-frame as

- $\vec{R}$ denotes the accelerometer position vector from O_I to the accelerometer P. $\vec{R}$ is represented in inertial frame, which is denoted as $\vec{R}^i$.
- $\vec{r}$ denotes the vehicle position vector from O_I to the center of the six-accelerometer scheme o_b. $\vec{r}$ is represented in body frame, which is denoted as $\vec{r}^b$.
- $\vec{\rho}$ denotes the accelerometer position vector from the center of the six-accelerometer scheme o_b to the accelerometer P. $\vec{\rho}$ is represented in body-frame, which is denoted as $\vec{\rho}^b$.

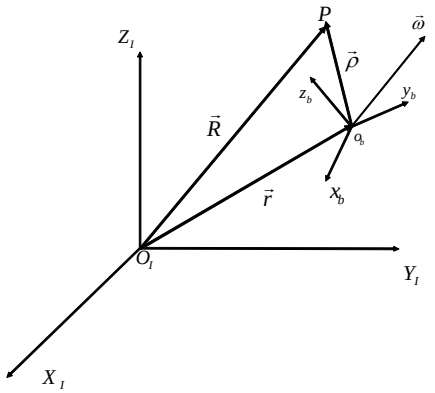

Fig. 1. Geometry of the body-frame (b) and the inertial-frame (I).

The vehicle position $\vec{r}$ can be represented in inertial frame through transformation matrix C_b^i, that is

$$\vec{r}^{\,i} = C_b^i \vec{r}^{\,b}. \tag{2}$$

Form (2), the position equation is yielded as

$$\vec{v}^{\,i} = C_b^i \left(\vec{v}^{\,b} + \vec{\omega}_{ib}^{\,b} \times \vec{r}^{\,b} \right). \tag{3}$$

2.3. Velocity equation

The six-accelerometer configuration is shown as Fig. 2, and the positional vector and sensitive vector of each accelerometer are shown as Table 1. According to Chen's paper, the six-accelerometer INS dynamic equation that considers the attitude and gravitation $\vec{G}^i$ effects will be rewritten as

$$\begin{bmatrix} \dot{\vec{\omega}}_{ib}^{\,b} \\ C_i^b \dot{\vec{v}}^{\,i} \end{bmatrix} = \frac{1}{2} \begin{bmatrix} S/\rho \\ T \end{bmatrix} A + \rho \begin{bmatrix} 0 \\ 0 \\ 0 \\ \omega_y \omega_z \\ \omega_x \omega_z \\ \omega_x \omega_y \end{bmatrix}, \tag{4}$$

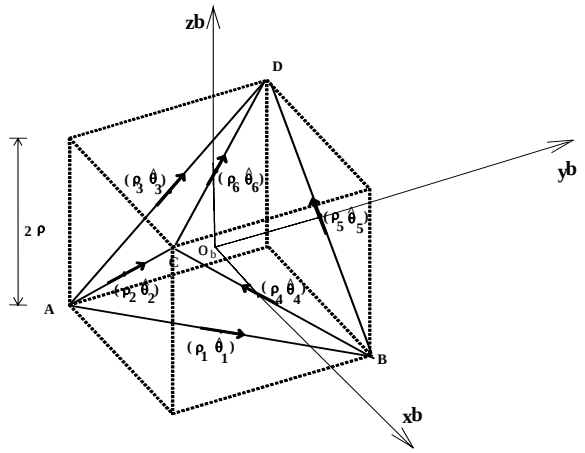

Fig. 2. Six-accelerometer scheme.

Table 1. Position and sensitive vectors of the six accelerometers.

No.	Position vector	Sensitive vector
1	$\vec{\rho}_1 = \begin{bmatrix} 0 & 0 & -\rho \end{bmatrix}^T$	$\vec{\theta}_1 = \frac{1}{\sqrt{2}} \begin{bmatrix} 1 & 1 & 0 \end{bmatrix}^T$
2	$\vec{\rho}_2 = \begin{bmatrix} 0 & -\rho & 0 \end{bmatrix}^T$	$\vec{\theta}_2 = \frac{1}{\sqrt{2}} \begin{bmatrix} 1 & 0 & 1 \end{bmatrix}^T$
3	$\vec{\rho}_3 = \begin{bmatrix} -\rho & 0 & 0 \end{bmatrix}^T$	$\vec{\theta}_3 = \frac{1}{\sqrt{2}} \begin{bmatrix} 0 & 1 & 1 \end{bmatrix}^T$
4	$\vec{\rho}_4 = \begin{bmatrix} \rho & 0 & 0 \end{bmatrix}^T$	$\vec{\theta}_4 = \frac{1}{\sqrt{2}} \begin{bmatrix} 0 & -1 & 1 \end{bmatrix}^T$
5	$\vec{\rho}_5 = \begin{bmatrix} 0 & \rho & 0 \end{bmatrix}^T$	$\vec{\theta}_5 = \frac{1}{\sqrt{2}} \begin{bmatrix} -1 & 0 & 1 \end{bmatrix}^T$
6	$\vec{\rho}_6 = \begin{bmatrix} 0 & 0 & \rho \end{bmatrix}^T$	$\vec{\theta}_6 = \frac{1}{\sqrt{2}} \begin{bmatrix} -1 & 1 & 0 \end{bmatrix}^T$

where

- $A_j = s_j + C_i^b \vec{G}^i \cdot \vec{\theta}_j$; $j = 1, \cdots, 6$,
- s_j is the measurement of accelerometer j,
- ρ is the distance from the body-frame origin to each accelerometer,
- $A = \begin{bmatrix} A_1 & A_2 & A_3 & A_4 & A_5 & A_6 \end{bmatrix}^T$ is the acceleration array,
- $S = \frac{1}{\sqrt{2}} \begin{bmatrix} 1 & -1 & 0 & 0 & 1 & -1 \\ -1 & 0 & 1 & -1 & 0 & -1 \\ 0 & 1 & -1 & -1 & 1 & 0 \end{bmatrix}$ is the position matrix,
- $T = \frac{1}{\sqrt{2}} \begin{bmatrix} 1 & 1 & 0 & 0 & -1 & -1 \\ 1 & 0 & 1 & -1 & 0 & 1 \\ 0 & 1 & 1 & 1 & 1 & 0 \end{bmatrix}$ is the orientation matrix.

From (4), the velocity equation is

$$\dot{\vec{v}}^{\,i} = C_b^i \left(\frac{1}{2} TA + \rho \begin{bmatrix} \omega_y \omega_z \\ \omega_x \omega_z \\ \omega_x \omega_y \end{bmatrix} \right). \tag{5}$$

The transformation matrix C_i^b can be found from (1).

2.4. Angular rate equation

From (4), the angular rate is

$$\dot{\vec{\omega}}_{ib}^{\,b} = \frac{1}{2} S/\rho \, A. \tag{6}$$

3. ERROR EQUATION

The errors of the system of six-accelerometer INS involve bias, misalignment and electronic counting errors. We will depict in detail for the error equations of a six-accelerometer INS in this paper.

3.1. Attitude error equation

The attitude of a vehicle is dependent on the time derivative of the direction cosine matrix (1). The relationship between computed transformation matrix $\hat{C}_b^i$ and ideal transformation matrix C_b^i is [7]

$$\hat{C}_b^i = \left(I - \left[\vec{\phi}\times\right]\right)C_b^i . \tag{7}$$

By defining

$$\delta C_b^i = -\left[\vec{\phi}\times\right]C_b^i , \quad \hat{\omega}_{ib}^b = \vec{\omega}_{ib}^b + \delta\vec{\omega}_{ib}^b .$$

The attitude error equation can be yielded as

$$\dot{\vec{\phi}} = -C_b^i \delta\vec{\omega}_{ib}^b . \tag{8}$$

3.2. Position error equation

The computed velocity is assumed as the summation of error and ideal velocity, that is

$$\dot{\vec{r}}_c^i = \vec{v}_t^i + \delta\vec{v}^i . \tag{9}$$

From the above equation, the position error equation is

$$\delta\dot{\vec{r}}^i = \delta\vec{v}^i . \tag{10}$$

3.3. Velocity error equation

By assuming the computed velocity equation (5) is the summation of error and ideal velocity. It is $\vec{v}_c^i = \vec{v}_t^i + \delta\vec{v}^i$. The accelerometer measurement is the summation of ideal measurement and noise. It is $s_c = s_t + \delta s$.

The computed velocity equation is written as

$$\dot{\vec{v}}_c^i = \left(C_b^i + \delta C_b^i\right)\left(\frac{1}{2}T\left(s_t + g_t + \delta s + \delta g\right) + \vec{\omega}_t^2 + \delta\vec{\omega}^2\right), \tag{11}$$

where

$$\vec{\omega}^2 = \left[\omega_y\omega_z \quad \omega_x\omega_z \quad \omega_x\omega_y\right]^T ,$$

$$\delta\vec{\omega}^2 = \left[\omega_y\delta\omega_z + \omega_z\delta\omega_y \quad \omega_x\delta\omega_z + \omega_z\delta\omega_x \quad \omega_x\delta\omega_y + \omega_y\delta\omega_x\right]^T ,$$

$$\delta g = \left[\delta g_1 \quad \delta g_2 \quad \delta g_3 \quad \delta g_4 \quad \delta g_5 \quad \delta g_6\right]^T ,$$

$$\delta g_j = \delta C_i^b \vec{G}^i \cdot \vec{\theta}_j .$$

From the above equation the velocity error equation is

$$\begin{aligned}\delta\dot{\vec{v}}^i = {} & C_b^i\left(\frac{1}{2}T\left(s_t + g_t\right) + \vec{\omega}_t^2\right)\times\vec{\phi} \\ & + C_b^i\left(\frac{1}{2}T\left(\delta s + \delta g\right) + \delta\vec{\omega}^2\right).\end{aligned} \tag{12}$$

3.4. Angular velocity error equation

Similar to above derivation, it can find the error equation of angular velocity, that is

$$\delta\dot{\vec{\omega}}_{ib}^b = \frac{1}{2\rho}S\left(\delta s + \delta g\right). \tag{13}$$

4. SCHEME CALIBRATION

The navigation error of six-accelerometer INS involves the bias, scale factor and misalignment which contain orientation and location error. The orientation error, bias and scale factor of each accelerometer will be determined by the orientation calibration which uses the gravity effect. The key element in orientation calibration is that the sensitive axes of each accelerometer must be linearly independent. We divide six accelerometers into two sets that are set $\left[\vec{\theta}_2^b \quad \vec{\theta}_3^b \quad \vec{\theta}_5^b\right]$ and set $\left[\vec{\theta}_1^b \quad \vec{\theta}_4^b \quad \vec{\theta}_6^b\right]$, and then calibrate each set to get the error parameters. The location error $\Delta\vec{\rho}$ will be determined by the location calibration which uses the centripetal force effect.

4.1. Orientation calibration

$C_a^{a'}$ is a transformation matrix which is used to convert the ideal sensitive axes into the realistic sensitive axes. The transformation matrix of set $\left[\vec{\theta}_2^b \quad \vec{\theta}_3^b \quad \vec{\theta}_5^b\right]$ is defined as

$$C_a^{a'} = \begin{bmatrix} 1 & \Delta\beta_{xz} & -\Delta\beta_{xy} \\ -\Delta\beta_{yz} & 1 & \Delta\beta_{yx} \\ \Delta\beta_{zy} & -\Delta\beta_{zx} & 1 \end{bmatrix}. \tag{14}$$

For set $\left[\vec{\theta}_1^b \quad \vec{\theta}_4^b \quad \vec{\theta}_6^b\right]$, the transformation matrix is defined as

$$C_a^{a'} = \begin{bmatrix} 1 & \Delta\alpha_{xz} & -\Delta\alpha_{xy} \\ -\Delta\alpha_{yz} & 1 & \Delta\alpha_{yx} \\ \Delta\alpha_{zy} & -\Delta\alpha_{zx} & 1 \end{bmatrix}. \tag{15}$$

When the six-accelerometer INS bears the specific force $\vec{a}^b = \left[a_x \quad a_y \quad a_z\right]^T$, the accelerometer outputs are expressed as an analog electrical signal P_{aj} that relates to the scale factor SF_{aj} and bias b_{aj}, $j = 1\cdots6$. The equations of analog electrical signal P_{aj} are shown as

$$\begin{aligned}P_{a1} = SF_{a1}(T)\int_0^T\Bigg(b_{a1}(T) + \frac{1}{\sqrt{2}}\Big[\left(1+\Delta\alpha_{xy}\right)a_x \\ + \left(1-\Delta\alpha_{xy}-\Delta\alpha_{xz}\right)a_y + \Delta\alpha_{xz}a_z\Big]\Bigg)dt ,\end{aligned} \tag{16a}$$

$$P_{a2} = SF_{a2}(T)\int_0^T\Bigg(b_{a2}(T) + \frac{1}{\sqrt{2}}\Big[\left(1+\Delta\beta_{xy}\right)a_x^b$$

$$+\Delta\beta_{xz}a_y^b+\left(1+\Delta\beta_{xz}-\Delta\beta_{xy}\right)a_z^b\Big]\Big)dt\,, \tag{16b}$$

$$P_{a3}=SF_{a3}(T)\int_0^T\Big(b_{a3}(T)+\frac{1}{\sqrt{2}}\Big[-\left(\Delta\beta_{yz}+\Delta\beta_{yx}\right)a_x^b + a_y^b+\left(1+\Delta\beta_{yx}-\Delta\beta_{yz}\right)a_z^b\Big]\Big)dt\,, \tag{16c}$$

$$P_{a4}=SF_{a4}(T)\int_0^T\Big(b_{a4}(T)+\frac{1}{\sqrt{2}}\Big[-\left(\Delta\alpha_{yz}+\Delta\alpha_{yx}\right)a_x -\left(1+\Delta\alpha_{yz}-\Delta\alpha_{yx}\right)a_y+a_z\Big]\Big)dt\,, \tag{16d}$$

$$P_{a5}=SF_{a5}(T)\int_0^T\Big(b_{a5}(T)+\frac{1}{\sqrt{2}}\Big[-\left(1-\Delta\beta_{zy}\right)a_x^b - \Delta\beta_{zx}a_y^b+\left(1-\Delta\beta_{zx}+\Delta\beta_{zy}\right)a_z^b\Big]\Big)dt\,, \tag{16e}$$

$$P_{a6}=SF_{a6}(T)\int_0^T\Big(b_{a6}(T)+\frac{1}{\sqrt{2}}\Big[-\left(1-\Delta\alpha_{zy}\right)a_x +\left(1+\Delta\alpha_{zy}+\Delta\alpha_{zx}\right)a_y-\Delta\alpha_{zx}a_z\Big]\Big)dt\,. \tag{16f}$$

In the multi-attitude static test the scale factor, biases and orientation error can be determined by the gravity effect. For the set $\left[\vec{\theta}_2^b \quad \vec{\theta}_3^b \quad \vec{\theta}_5^b\right]$ with twelve error parameters, at least six attitudes are requested to measure eighteen sensors' output for determining the error parameters. The six attitudes are shown as Table 2. By (16b), (16c), (16e) and Table 2, there are eighteen output equations which P_{aij} can be obtained, where the index i is the accelerometer number and index j is the attitude number. From the eighteen output equations, the scale factors are found as

Table 2. Six attitudes for the set $\left[\vec{\theta}_2^b \quad \vec{\theta}_3^b \quad \vec{\theta}_5^b\right]$.

No.	Attitude	No.	Attitude
1	$\vec{a}_{b1}=\frac{g}{\sqrt{2}}\left[-1 \quad 0 \quad 1\right]^T$	4	$\vec{a}_{b4}=-\frac{g}{\sqrt{2}}\left[1 \quad 0 \quad 1\right]^T$
2	$\vec{a}_{b2}=-\frac{g}{\sqrt{2}}\left[-1 \quad 0 \quad 1\right]^T$	5	$\vec{a}_{b5}=\frac{g}{\sqrt{2}}\left[0 \quad 1 \quad 1\right]^T$
3	$\vec{a}_{b3}=\frac{g}{\sqrt{2}}\left[1 \quad 0 \quad 1\right]^T$	6	$\vec{a}_{b6}=-\frac{g}{\sqrt{2}}\left[0 \quad 1 \quad 1\right]^T$

Table 3. Six attitudes for the set $\left[\vec{\theta}_1^b \quad \vec{\theta}_4^b \quad \vec{\theta}_6^b\right]$.

No.	Attitude	No.	Attitude
1	$\vec{a}_{b1}=\frac{g}{\sqrt{2}}\left[0 \quad -1 \quad 1\right]^T$	4	$\vec{a}_{b4}=-\frac{g}{\sqrt{2}}\left[1 \quad 1 \quad 0\right]^T$
2	$\vec{a}_{b2}=-\frac{g}{\sqrt{2}}\left[0 \quad -1 \quad 1\right]^T$	5	$\vec{a}_{b5}=\frac{g}{\sqrt{2}}\left[-1 \quad 1 \quad 0\right]^T$
3	$\vec{a}_{b3}=\frac{g}{\sqrt{2}}\left[1 \quad 1 \quad 0\right]^T$	6	$\vec{a}_{b6}=-\frac{g}{\sqrt{2}}\left[-1 \quad 1 \quad 0\right]^T$

$$SF_{a2}(T)=\frac{\left(P_{a21}-P_{a22}\right)+3\left(P_{a23}-P_{a24}\right)-2\left(P_{a25}-P_{a26}\right)}{4gT}, \tag{17a}$$

$$SF_{a3}(T)=\frac{-\left(P_{a31}-P_{a32}\right)-\left(P_{a33}-P_{a34}\right)+2\left(P_{a35}-P_{a36}\right)}{2gT}, \tag{17b}$$

$$SF_{a5}(T)=\frac{3\left(P_{a51}-P_{a52}\right)+\left(P_{a53}-P_{a54}\right)-2\left(P_{a55}-P_{a56}\right)}{4gT}. \tag{17c}$$

Substituting the above equations into the eighteen output equations, the bias and orientation error can be determined by the least square method.

Similar to above derivation, the six attitudes for the set $\left[\vec{\theta}_1^b \quad \vec{\theta}_4^b \quad \vec{\theta}_6^b\right]$ are shown as Table 3. The scale factors for the set $\left[\vec{\theta}_1^b \quad \vec{\theta}_4^b \quad \vec{\theta}_6^b\right]$ are

$$SF_{a1}(T)=\frac{2\left(P_{a11}-P_{a12}\right)+3\left(P_{a13}-P_{a14}\right)+\left(P_{a15}-P_{a16}\right)}{4gT}, \tag{18a}$$

$$SF_{a4}(T)=\frac{2\left(P_{a41}-P_{a42}\right)+\left(P_{a43}-P_{a44}\right)+\left(P_{a45}-P_{a46}\right)}{2gT}, \tag{18b}$$

$$SF_{a6}(T)=\frac{2\left(P_{a61}-P_{a62}\right)+\left(P_{a63}-P_{a64}\right)+3\left(P_{a65}-P_{a66}\right)}{4gT}. \tag{18c}$$

The bias and orientation error can be determined by the least square method from the eighteen output equations.

4.2. The location calibration

Assuming the real position vector of each accelerometer is shown as

$$\vec{\rho}_j^{\,*}=\vec{\rho}_j+\Delta\vec{\rho}_j\,,\quad j=1\cdots6\,, \tag{19}$$

where

- $\vec{\rho}_j$ is ideal position vector of accelerometer j, which is shown as table 1,
- $\Delta\vec{\rho}_j\equiv\left[\Delta x_j \quad \Delta y_j \quad \Delta z_j\right]^T$ is defined as the position error vector of accelerometer j.

Each accelerometer will be generated three centripetal forces by the angular rates in *x*, *y* and *z* axes respectively. Through comparing the differences between the ideal and measurement outputs of six accelerometers we can obtain the location error. By centripetal force accelerometer j can sense the acceleration.

$$\vec{f}_j^{\,b*}=\vec{\omega}_{ib}^b\times\vec{\omega}_{ib}^b\times\vec{\rho}_j^{\,b*}-C_i^b\vec{G}^i\,. \tag{20}$$

The output of each accelerometer is represented as

$$P_{aj} = SF_{aj}\left(\vec{f}_j^{b*} \cdot \vec{\theta}_j + b_{aj}\right). \quad (21)$$

We can determine the location errors when three angular rates test in laboratory is completed.

5. COMPENSATOR DESIGN

In this section, we propose a compensator to compensate misalignment of six-accelerometer INS. The compensator scheme is based on location and orientation errors.

Considering the position error effect, the measured specific forces $\vec{f}_j^{b*}$, $j = 1 \cdots 6$ firstly, and

$$\vec{f}_j^{b*} = \vec{f}_j^{b} + \Delta\vec{f}_j^{b}, \quad (22)$$

where

- $\vec{f}_j^{b} = C_i^b \dot{\vec{v}}^i + \vec{\omega}_{ib}^b \times \vec{\omega}_{ib}^b \times \vec{\rho}_j + \dot{\vec{\omega}}_{ib}^b \times \vec{\rho}_j - C_i^b \vec{G}^i$,
- $\Delta\vec{f}_j^{b} = \vec{\omega}_{ib}^b \times \vec{\omega}_{ib}^b \times \Delta\vec{\rho}_j + \dot{\vec{\omega}}_{ib}^b \times \Delta\vec{\rho}_j$,
- $\vec{f}_j^{b}$ is the ideal specific force of accelerometer j,
- $\Delta\vec{f}_j^{b}$ is the specific force error, which are all in body-frame.

The accelerometer output measurement must consider the orientation error effect. The measurements s^* of the accelerometers are represented by ideal measurements and transformation matrices. The measurements s^* of set $\left[\vec{\theta}_2^b \quad \vec{\theta}_3^b \quad \vec{\theta}_5^b\right]$ and $\left[\vec{\theta}_1^b \quad \vec{\theta}_4^b \quad \vec{\theta}_6^b\right]$ are written as

$$\begin{bmatrix} s_2^* \\ s_3^* \\ s_5^* \end{bmatrix} = \begin{bmatrix} 1 & \Delta\beta_{xz} & -\Delta\beta_{xy} \\ -\Delta\beta_{yz} & 1 & \Delta\beta_{yx} \\ \Delta\beta_{zy} & -\Delta\beta_{zx} & 1 \end{bmatrix} \begin{bmatrix} s_2 \\ s_3 \\ s_5 \end{bmatrix}, \quad (23)$$

$$\begin{bmatrix} s_1^* \\ s_4^* \\ s_6^* \end{bmatrix} = \begin{bmatrix} 1 & \Delta\alpha_{xz} & -\Delta\alpha_{xy} \\ -\Delta\alpha_{yz} & 1 & \Delta\alpha_{yx} \\ \Delta\alpha_{zy} & -\Delta\alpha_{zx} & 1 \end{bmatrix} \begin{bmatrix} s_1 \\ s_2 \\ s_3 \end{bmatrix}. \quad (24)$$

Misalignment error involves orientation and location error. The measurement of accelerometer with misalignment is represented as s^{**}. The measurements s^{**} of set $\left[\vec{\theta}_2^b \quad \vec{\theta}_3^b \quad \vec{\theta}_5^b\right]$ and $\left[\vec{\theta}_1^b \quad \vec{\theta}_4^b \quad \vec{\theta}_6^b\right]$ should be written as

$$\begin{bmatrix} s_2^{**} \\ s_3^{**} \\ s_5^{**} \end{bmatrix} = \begin{bmatrix} s_2^{*} \\ s_3^{*} \\ s_5^{*} \end{bmatrix} + \begin{bmatrix} 1 & \Delta\beta_{xz} & -\Delta\beta_{xy} \\ -\Delta\beta_{yz} & 1 & \Delta\beta_{yx} \\ \Delta\beta_{zy} & -\Delta\beta_{zx} & 1 \end{bmatrix} \begin{bmatrix} \Delta\vec{f}_2^b \cdot \vec{\theta}_2 \\ \Delta\vec{f}_3^b \cdot \vec{\theta}_3 \\ \Delta\vec{f}_5^b \cdot \vec{\theta}_5 \end{bmatrix}, \quad (25)$$

$$\begin{bmatrix} s_1^{**} \\ s_4^{**} \\ s_6^{**} \end{bmatrix} = \begin{bmatrix} s_1^{*} \\ s_4^{*} \\ s_6^{*} \end{bmatrix} + \begin{bmatrix} 1 & \Delta\alpha_{xz} & -\Delta\alpha_{xy} \\ -\Delta\alpha_{yz} & 1 & \Delta\alpha_{yx} \\ \Delta\alpha_{zy} & -\Delta\alpha_{zx} & 1 \end{bmatrix} \begin{bmatrix} \Delta\vec{f}_1^b \cdot \vec{\theta}_1 \\ \Delta\vec{f}_4^b \cdot \vec{\theta}_4 \\ \Delta\vec{f}_6^b \cdot \vec{\theta}_6 \end{bmatrix}. \quad (26)$$

5.1. Location compensation

From (23)-(26) we can know that the compensation design is an algorithm with sequence. First, it is location compensation to get the output s^*. Second, it is orientation compensation to get the ideal output s.

The location compensation outputs s_j^* can be found from (25) and (26)

$$\begin{bmatrix} s_2^{*} \\ s_3^{*} \\ s_5^{*} \end{bmatrix} = \begin{bmatrix} s_2^{**} \\ s_3^{**} \\ s_5^{**} \end{bmatrix} - \begin{bmatrix} 1 & \Delta\beta_{xz} & -\Delta\beta_{xy} \\ -\Delta\beta_{yz} & 1 & \Delta\beta_{yx} \\ \Delta\beta_{zy} & -\Delta\beta_{zx} & 1 \end{bmatrix} \begin{bmatrix} \Delta\vec{f}_2^b \cdot \vec{\theta}_2 \\ \Delta\vec{f}_3^b \cdot \vec{\theta}_3 \\ \Delta\vec{f}_5^b \cdot \vec{\theta}_5 \end{bmatrix}, \quad (27)$$

$$\begin{bmatrix} s_1^{*} \\ s_4^{*} \\ s_6^{*} \end{bmatrix} = \begin{bmatrix} s_1^{**} \\ s_4^{**} \\ s_6^{**} \end{bmatrix} - \begin{bmatrix} 1 & \Delta\alpha_{xz} & -\Delta\alpha_{xy} \\ -\Delta\alpha_{yz} & 1 & \Delta\alpha_{yx} \\ \Delta\alpha_{zy} & -\Delta\alpha_{zx} & 1 \end{bmatrix} \begin{bmatrix} \Delta\vec{f}_1^b \cdot \vec{\theta}_1 \\ \Delta\vec{f}_4^b \cdot \vec{\theta}_4 \\ \Delta\vec{f}_6^b \cdot \vec{\theta}_6 \end{bmatrix}. \quad (28)$$

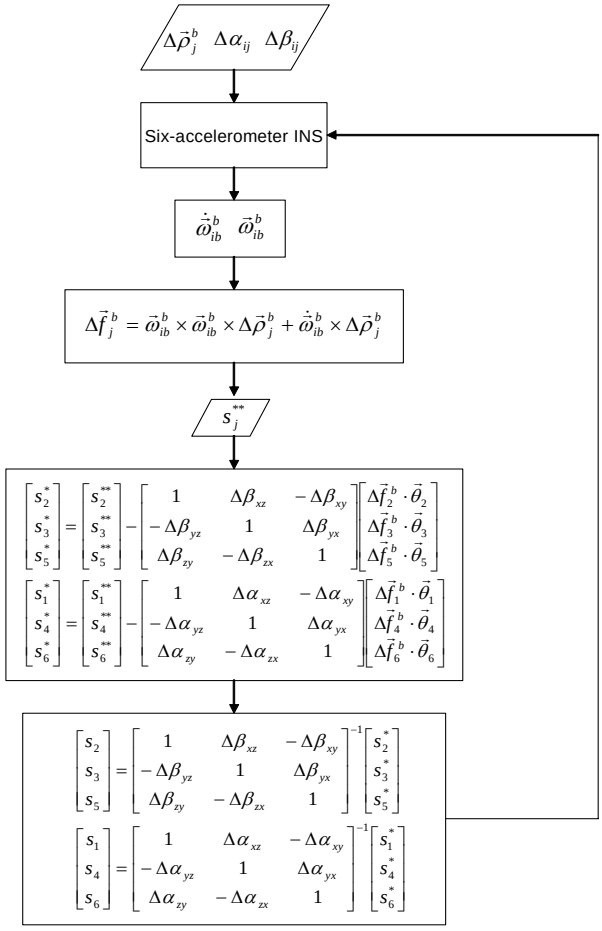

Fig. 3. Six-accelerometer INS compensator.

5.2. Orientation compensation

The orientation compensation output s_j can be found from (23) and (24)

$$\begin{bmatrix} s_2 \\ s_3 \\ s_5 \end{bmatrix} = \begin{bmatrix} 1 & \Delta\beta_{xz} & -\Delta\beta_{xy} \\ -\Delta\beta_{yz} & 1 & \Delta\beta_{yx} \\ \Delta\beta_{zy} & -\Delta\beta_{zx} & 1 \end{bmatrix}^{-1} \begin{bmatrix} s_2^* \\ s_3^* \\ s_5^* \end{bmatrix}, \quad (29)$$

$$\begin{bmatrix} s_1 \\ s_4 \\ s_6 \end{bmatrix} = \begin{bmatrix} 1 & \Delta\alpha_{xz} & -\Delta\alpha_{xy} \\ -\Delta\alpha_{yz} & 1 & \Delta\alpha_{yx} \\ \Delta\alpha_{zy} & -\Delta\alpha_{zx} & 1 \end{bmatrix}^{-1} \begin{bmatrix} s_1^* \\ s_4^* \\ s_6^* \end{bmatrix}. \quad (30)$$

The compensator flow chart is shown as Fig. 3.

The specific force errors could be obtained by (22) and decreased by designed compensator. Thus the correct angular rate and angular acceleration are calculated by (6). Since the computed errors of angular rate and angular acceleration can't be obtained by calibration in laboratory. The designed compensator in this paper ignores the effects of angular rate and angular acceleration errors.

6. EXPERIMENT OF ORIENTATION CALIBRATION

This calibration experiment divides two sets, $\begin{bmatrix} \vec{\theta}_2^b & \vec{\theta}_3^b & \vec{\theta}_5^b \end{bmatrix}$ and $\begin{bmatrix} \vec{\theta}_1^b & \vec{\theta}_4^b & \vec{\theta}_6^b \end{bmatrix}$. Through the experiments of Table 2 and Table 3, we can get the measurement outputs P_a. The scale factor SF_a, bias b_a and orientation errors $\Delta\alpha$, $\Delta\beta$ can be obtained by the P_a.

6.1. Experiment setting

In this experiment, it designs and manufactures a six-accelerometer inertial measurement unit (IMU) which is shown as Fig. 4. The IMU fixes onto an index table that is shown as Fig. 5. When changing the index table, it will cause the IMU attitude changing. The six-accelerometer scheme can sense the gravity. We choose type QA-1100 accelerometer for this experiment, and its accuracy is 10milli-g but the index table can reach 5 μg for its accuracy. Thus, the index table can be satisfied for the experiment requirement. The orientation calibration is shown as Fig. 6.

6.2. Experiment result

In this orientation calibration experiment we got measurement data of two sets which are $\begin{bmatrix} \vec{\theta}_2^b & \vec{\theta}_3^b & \vec{\theta}_5^b \end{bmatrix}$ and $\begin{bmatrix} \vec{\theta}_1^b & \vec{\theta}_4^b & \vec{\theta}_6^b \end{bmatrix}$. Because the measurement is random signal, each experiment set takes 1000 data and its mean value. The mean values for the set $\begin{bmatrix} \vec{\theta}_2^b & \vec{\theta}_3^b & \vec{\theta}_5^b \end{bmatrix}$ and set $\begin{bmatrix} \vec{\theta}_1^b & \vec{\theta}_4^b & \vec{\theta}_6^b \end{bmatrix}$ are shown as Table 4 and Table 5 respectively. Those are the measurement outputs P_a, which are used to compute the scalar factors, bias and orientation errors, whose parameters are shown as Table 6.

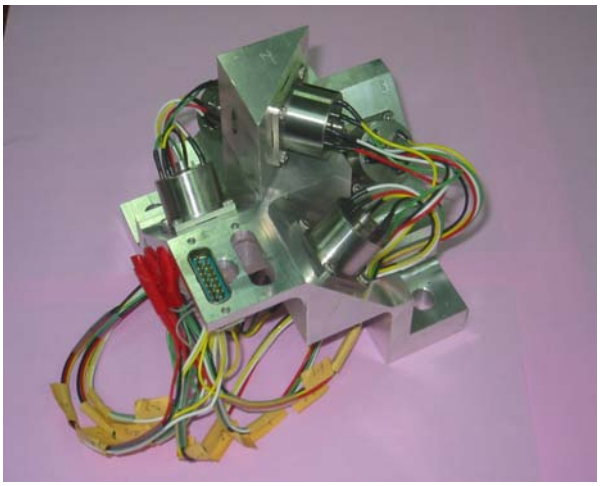

Fig. 4. The six-accelerometer IMU.

Fig. 5. The index table.

Fig. 6. The orientation calibration experiment.

Table 4. Measurement outputs of set $\left[\vec{\theta}_2^b \quad \vec{\theta}_3^b \quad \vec{\theta}_5^b\right]$.

No.	Mean Value	No.	Mean Value	No.	Mean Value
P_{a21}	-0.007018	P_{a31}	0.245359	P_{a51}	0.331528
P_{a22}	0.006972	P_{a32}	-0.244733	P_{a52}	-0.332370
P_{a23}	0.332051	P_{a33}	0.256841	P_{a53}	0.007012
P_{a24}	-0.332073	P_{a34}	-0.256300	P_{a54}	-0.007847
P_{a25}	0.161815	P_{a35}	0.501647	P_{a55}	0.162355
P_{a26}	-0.162231	P_{a36}	-0.500211	P_{a56}	-0.162492

Table 5. Measurement outputs of set $\left[\vec{\theta}_1^b \quad \vec{\theta}_4^b \quad \vec{\theta}_6^b\right]$.

No.	Mean Value	No.	Mean Value	No.	Mean Value
P_{a11}	-0.244244	P_{a41}	2.477090	P_{a61}	-1.222367
P_{a12}	0.243037	P_{a42}	-2.513921	P_{a62}	1.201903
P_{a13}	0.498045	P_{a43}	-1.235199	P_{a63}	-0.072459
P_{a14}	-0.498593	P_{a44}	1.193924	P_{a64}	0.047823
P_{a15}	0.011830	P_{a45}	-1.303769	P_{a65}	2.466940
P_{a16}	-0.012314	P_{a46}	1.262526	P_{a66}	-2.491551

6.3. Navigation error simulation

According to Table 6, a navigation simulation is designed to demonstrate the compensation effect. The accelerometer random error is assumed as 1milli-g and the vehicle motion with linear acceleration is $\ddot{\vec{r}}^i = \left[g \quad 0 \quad 0\right]^T$ m/sec^2. Initial vehicle motion is zero. Dynamic states of vehicle can be represented by six-accelerometer scheme output.

Before compensation, the errors of vehicle acceleration are shown as Figs. 7 and 8 for linear and angular acceleration respectively. The linear acceleration errors are bounded about -8 m/sec^2 ~ 2 m/sec^2 and angular acceleration errors are bounded about -0.1 rad/sec^2 ~ 0.5 rad/sec^2.

After compensation, the errors of vehicle acceleration are shown as Figs. 9 and 10 for linear and angular acceleration respectively. The linear acceleration errors are bounded about -0.002 m/sec^2 ~ 0.003 m/sec^2 and angular acceleration errors are bounded about -0.003 rad/sec^2 ~ 0.003 rad/sec^2.

According to the result in navigation error simulation, the linear and angular acceleration errors after compensation are less about two order than those before compensation. If the six-accelerometer mechanism had been calibrated, the effect of

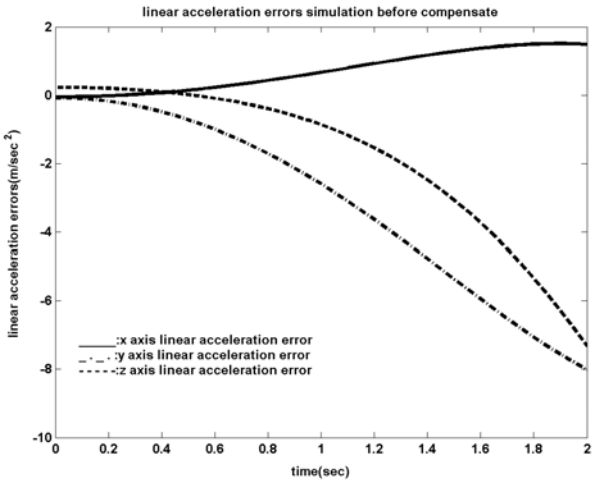

Fig. 7. Linear acceleration errors before compensation.

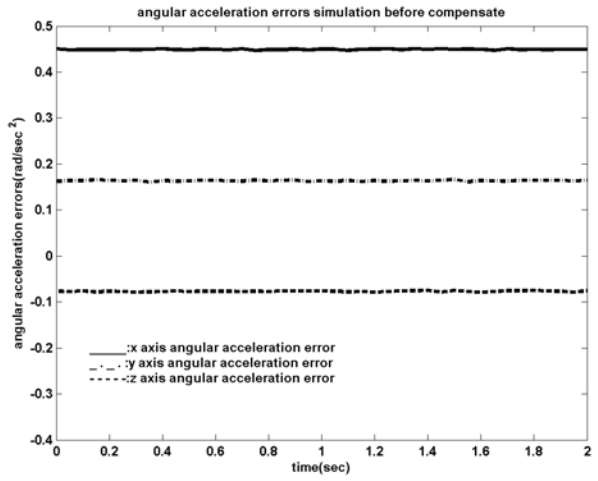

Fig. 8. Angular acceleration errors before compensation.

Table 6. The determined parameters.

Scalar factor(v/g)		bias(g)		Orientation error (Degree)			
SF_{a2}	0.332572	b_{a2}	-0.000242	$\Delta\beta_{xy}$	1.117319	$\Delta\beta_{yz}$	-0.738742
SF_{a3}	0.500242	b_{a3}	0.000867	$\Delta\beta_{xz}$	-0.175730	$\Delta\beta_{zx}$	2.454457
SF_{a5}	0.339215	b_{a5}	-0.000891	$\Delta\beta_{yx}$	-0.581196	$\Delta\beta_{zy}$	2.482135
SF_{a1}	0.509874	b_{a1}	-0.000731	$\Delta\alpha_{xy}$	-2.654967	$\Delta\alpha_{yz}$	-0.737387
SF_{a4}	2.493301	b_{a4}	-0.007977	$\Delta\alpha_{xz}$	2.596778	$\Delta\alpha_{zx}$	0.119537
SF_{a6}	2.476663	b_{a6}	-0.004691	$\Delta\alpha_{yx}$	-0.838703	$\Delta\alpha_{zy}$	-1.451107

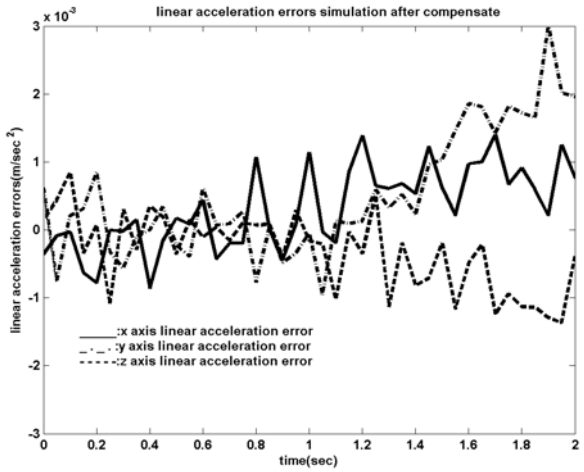

Fig. 9. Linear acceleration errors after compensation.

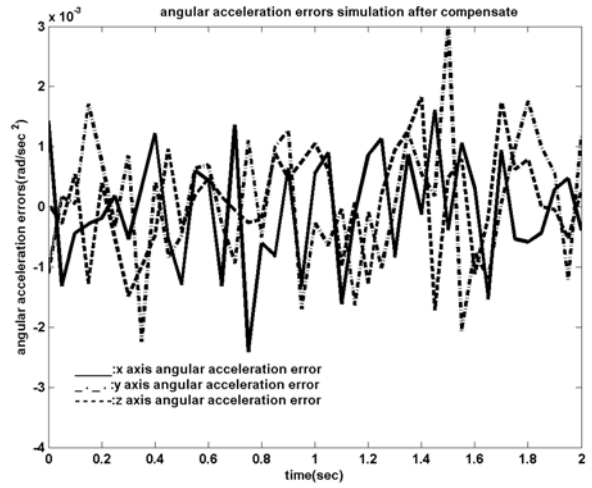

Fig. 10. Angular acceleration errors after compensation.

compensation could have reached a satisfied navigation results.

7. CONCLUSION

The navigation accuracy of the six-accelerometer INS depends on the misalignment. The six-accelerometer INS accuracy is increased by the designed compensator which can compensate the misalignment. According to the simulation results, it is shown that the angular acceleration error and the linear acceleration error are all bounded within a small range before compensation. The linear acceleration errors are more sensitive to time than the angular acceleration errors. In the future study, the six-accelerometer scheme will integrate with GPS to enhance navigation accuracy.

REFERENCES

[1] K. R. Britting, *Inertial Navigation System Analysis*, chap. 8, pp. 153-195, Wiley-Interscience, New York, 1971.

[2] C. F. O'Donnell, "Inertial navigation," *J. of the Franklin Institute*, vol. 266, no. 4-5, Oct.-Nov. 1958.

[3] A. R. Schuler, A. Grammatikos, and K. A. Fegler, "Measuring rotational motion with linear accelerometers," *IEEE Trans. on Aerospace and Electronic Systems*, vol. AES-3, no. 3, pp. 465-471, May 1967.

[4] J. H. Chen, S. C. Lee, and D. B. DeBra, "Gyroscope free strapdown inertial measurement unit by six liner accelerometers," *Journal of Guidance, Control, and Dynamics AIAA*, vol. 17, no. 2, pp. 286-290, March-April 1994.

[5] K. S. Mostov, *Design of Accelerometer-Base Gyro-Free Navigation System*, Ph.D. dissertation, Graduate Division of Engineering-Electrical Engineering and Computer Science University of California, Berkeley, chap. 5, pp. 178-225, 2000.

[6] W. Wrigley, W. M. Hollister, and W. G. Denhard, *Gyroscopic Theory, Design, and Instrumentation*, chap. 12, pp. 241-242, The Massachusetts Institute of Technology Press, 1969.

[7] K. R. Britting, *Inertial Navigation System Analysis*, chap. 6, pp. 86-91, Wiley-Interscience, New York, 1971.

Chao-Yu Hung received the B.S. from Chinese Military Academy in 1988 and the M.S. degree in Engineering Science from National Cheng Kung University 1996. He is currently working toward the Ph.D. degree at Department of System Engineering, Chung Cheng Institute of Technology, National Defense University, Taiwan, His research interests include Integrated Navigation System, INS, GPS, calibration and error analysis.

Chun-Min Fang received the B.S. and M.S. degrees in Mechanical Engineering from Chung Cheng Institute of Technology in 1988 and 1996 respectively. Since 2004, He is currently working toward the Ph.D. degree at Department of System Engineering, Chung Cheng Institute of Technology, National Defense University, Taiwan, His research interests include INS, calibration and error analysis.

Sou-Chen Lee received the B.S., M.S. and Ph.D. degrees in System Engineering from Chung Cheng Institute of Technology in 1979, 1985 and 1993 respectively. Since 2004, he has been a Dean of College of Electrical Engineering and Computer Science, Lunghwa University of Science and Technology. His research interests include dynamic system, INS and guidance.